WEIMOS: Creep of Rock Salt at Low Deviatoric Stresses

Christoph Lüdeling[1*], *Ralf-Michael Günther*[1], *Andreas Hampel*[2], *Junqing Sun-Kurczinski*[3], *Ralf Wolters*[3], *Uwe Düsterloh*[3], *Karl-Heinz Lux*[3], *Savaş Yıldırım*[4], *Dirk Zapf*[4], *Svenja Wacker*[5], *Ida Epkenhans*[5], *Joachim Stahlmann*[5], *Benjamin Reedlunn*[6]

[1]Institut für Gebirgsmechanik GmbH (IfG), Leipzig, Germany; [2]Hampel Consulting, Mainz, Germany; [3]Technische Universität Clausthal (TUC), Germany; [4]Leibniz Universität Hannover (LUH), Germany; [5]Technische Universität Braunschweig (TUBS), Germany; [6]Sandia National Laboratories, Albuquerque, NM, USA

* *christoph.luedeling@ifg-leipzig.de*

ABSTRACT: The vast majority of rock salt creep tests have been conducted at deviatoric stresses above 6 MPa, yet the long-term behaviour of waste repositories, mines and caverns is dominated by creep below 6 MPa. Steady-state creep in this range is very slow (around 10^{-6}/d or lower) and is easily overwhelmed by other effects, such as dilatancy and long transient phases. Hence, a careful experimental approach was developed to measure creep at low stresses that includes

- an isotropic compression step to consolidate the sample,
- high confining stresses to avoid dilating the sample during deviatoric stress steps,
- elevated temperature in the first deviatoric stress step to speed up transients,
- and several temperature steps to obtain several creep rates and activation energies from a single sample. Since dislocation microstructure depends only weakly on temperature, there are essentially no new transients in the later load stages.

We discuss the procedure in detail and present a long-term creep test (duration almost five years) at $4\ \mathrm{MPa}$ that validates the procedure. These tests should help calibrate rock salt constitutive models and derive parameter sets for creep laws, and hence allow them to predict long-term structural performance with greater confidence.

1 Introduction

The long-term behaviour of excavations in salt formations is dominated by creep at deviatoric stresses below, say, $6\ \mathrm{MPa}$. For waste repositories, in particular, this has implications for drift convergence (see e.g. Hampel et al. 2022) – which affects the behaviour of geotechnical barriers such as crushed salt backfill and drift seals – and for large-scale stress redistributions which affect the geological barrier by lowering the minor principal stress and possibly allow allowing fluid transport via pressure-driven percolation (see e.g. Kock et al. 2012).

However, experimental data is scarce in this region because creep tests on rock salt are predominantly conducted at higher stresses (see e.g. Salzer et al. 2015; Mellegard, Pfeifle 1993). Pioneering work on the creep of natural rock salt in the low-stress range has been done by Bérest et al (2017, 2020; see also Gharbi et al. 2020), but the amount of available data does not currently allow a comprehensive characterisation of the low-stress creep properties of specific rock salt varieties. Furthermore, considerable scatter and uncertainties exist, e.g. about pre-existing damage, the influence of external humidity and the question of stationarity. Nevertheless, it seems clear that rock salt creeps faster at low stress than would

be expected from a pure Norton-type creep law such as BGRa (Hunsche, Schulze 1995),

$$\dot{\epsilon}_{\mathrm{Norton}} = A\, e^{-\frac{Q}{RT}} \sigma^n, \qquad (1)$$

with $n = 5$. Figure 1 summarises stationary creep rates for some rock salt varieties in the range from $40\ \mathrm{MPa}$ to $0.1\ \mathrm{MPa}$. For stresses of a few MPa, creep rates generally are in the range of $\dot{\epsilon} \sim 10^{-6}/\mathrm{d}$ (i.e. around $10^{-11}/\mathrm{s}$).

This is consistent with microphysical analyses of creep mechanisms. At moderate and high stress, creep of rock salt is dominated by intracrystalline dislocation motion, with comparatively steep stress dependence. At lower stresses, it has been shown (Urai et al. 1986; Schleder, Urai 2005) that fluid-assisted dissolution-precipitation processes, such as pressure solution and dynamic recrystallization, become the main creep mechanisms. Spiers et al. (1990) derived the creep rate for pressure solution creep to be similar to Eq. (1), but with a linear stress dependence, i.e. $n = 1$.

While the stationary creep of rock salt has often been modelled using a single-component power law such as Eq. (1), current state-of-the-art constitutive models (see e.g. Lüdeling et al. 2018, Reedlunn et al. 2022) contain more complex creep laws that allow for enhanced creep rates at low stress. On the other hand, the lack of a proper experimental data base means that the creep laws can only be partially validated, and necessary parameters cannot be firmly determined.

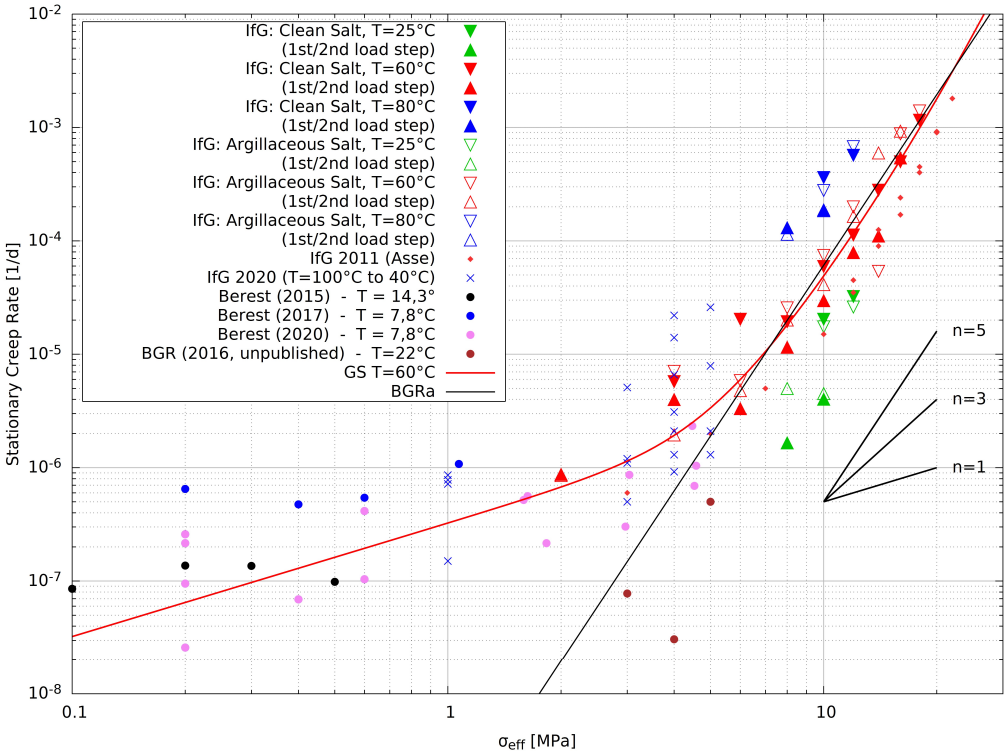


Figure 1: Stationary creep rates for various rock salt varieties (modified from Herchen et al. 2018). The triangles indicate measurements on WIPP salt from joint project III (Salzer et al. 2015). Note that the Bérest and BGR tests used different salt varieties. The solid lines indicate the BGRa law (black) and the Günther-Salzer model (three-component power law, red).

In the WEIMOS research project, creep at low stress is one of the work areas. In this paper, we present an improved creep test procedure to accurately determine creep rates and their temperature dependence at low stress.

2 Key Problems in and Strategies for Identifying "True" Creep

In lab tests, the stationary creep of rock salt, in particular for the small rates at low stresses, is easily overwhelmed by other effects, both from external influences and the internal structure of the salt. Generally, the disturbances will increase the measured creep rates, i.e. the stationary rates will be overestimated.

The mechanical disturbances during sample preparation generically introduce a small amount of dilatancy, generally in the order of $\epsilon \sim 10^{-3}$, to the specimen. Similarly, end face roughness with amplitude of a few hundredths of a millimetre corresponds to, for samples of length $120\,\mathrm{mm}$, a deformation in the range of $\epsilon \sim 10^{-4}$ to $\epsilon \sim 10^{-3}$. Note that for a (measured) creep rate of $\dot{\epsilon} = 10^{-6}/\mathrm{d}$, a spurious deformation of $\epsilon = 10^{-3}$ implies more than $10^3\,\mathrm{d}$ before the actual creep stage of the salt is reached.

In addition, a temperature fluctuation of $1\,\mathrm{K}$ corresponds to several weeks of creep at $\dot{\epsilon} \sim 10^{-6}/\mathrm{d}$; however this is a reversible effect and may be corrected for if one assumes the temperature fluctuation is uniform throughout the sample.

It is currently an open question whether rock salt forms micro-cracks (dilates) under low uniaxial compressive stresses. If it does, the dilation will contribute to the measured creep rate. Furthermore, if the sample is not shielded, humidity from the ambient air can access the interior of the specimen via (pre-existing or newly generated) micro-cracks and speed up any fluid-assisted creep processes (Hunsche, Schulze 2002; Bérest et al 2020).

Finally, the low rates mean that any transient stage takes a long time. (Note that "transient" and "stationary" creep phases are, in particular, a feature of the dislocation microstructure, while dissolution-precipitation creep plausibly does not have a pronounced transient stage.) Hence, creep tests will be very time-consuming, and it is nontrivial to ascertain that a stationary stage has been reached.

To address these problems, some general strategies have been developed:

The first is to perform creep tests in a triaxial setup with high confining stress, e.g. $20\,\mathrm{MPa}$. The triaxial cell will isolate the sample from external humidity and allow for controlled sample temperatures independent of the ambient conditions. The confining stress suppresses dilatancy generation during the creep stage.

Additionally, triaxial tests enable an initial isotropic consolidation phase to heal the pre-existing damage and crush the end face asperities. It was found in Günther et al. (2015) that consolidating the samples for ten days at $20\,\mathrm{MPa}$ greatly reduced the intersample scatter at deviatoric stresses above $10\,\mathrm{MPa}$. For lower deviatoric stresses, longer consolidation phases are to be expected.

To reduce the required test durations, it is recommended to exploit temperature effects. A higher temperature accelerates creep deformation and thus speeds up the transient phase,

such that the stationary stage is reached faster. Elevated temperatures are usually closer to the rock temperatures in mines, and many applications, such as disposal of heat-generating waste, require knowledge of the temperature dependence of stationary creep rates. Tests at different temperatures, or with several temperature stages, can be used to derive the activation energies.

As we discuss in the next two sections, an understanding of the basic creep mechanisms is helpful to develop suitable test procedures and to obtain reliable creep rates.

3 Procedure at Moderate and High Stress

We briefly discuss the procedure of Günther et al. (2015) to determine stationary rates at higher stresses, say, above $8\,\mathrm{MPa}$, where dislocation creep dominates. Hence, one can exploit the transient creep behaviour to obtain both upper and lower bounds for the stationary creep rate.

The key point is that transient creep reflects the evolution of the dislocation microstructure towards an equilibrium state that is determined by the applied stress. Thus, after a stress increase, creep rates are initially high and subsequently reduce (the sample hardens, normal transient creep). After a stress decrease, on the other hand, the material is over-hardened, so creep rates are initially low and increase over time (inverse transient creep). In other words, the stationary rate is approached from above and below in normal and inverse transient creep, respectively.

Thus, in a series of two-stage creep tests with unloading, e.g. at $18\,\mathrm{MPa} \rightarrow 16\,\mathrm{MPa}$ and $16\,\mathrm{MPa} \rightarrow 14\,\mathrm{MPa}$, both normal and inverse transient creep occur at $16\,\mathrm{MPa}$, and the creep rates bound the stationary rate from both sides (see Figure 2).

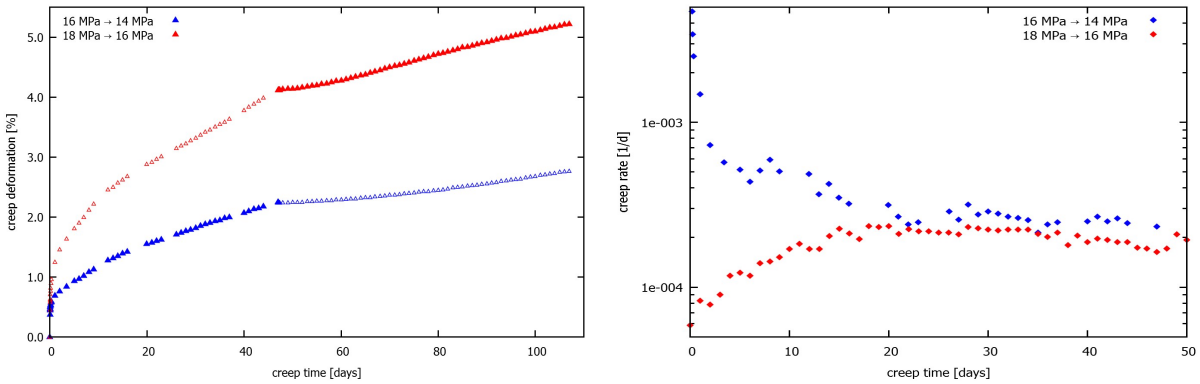


Figure 2: Determination of stationary creep rates (after Günther et al. 2015). Left panel: Deformation versus time for two-stage creep tests with $16\,\mathrm{MPa}$ and $14\,\mathrm{MPa}$ (blue, lower curve) and with $18\,\mathrm{MPa}$ and $16\,\mathrm{MPa}$ (red, upper curve). Note that the solid symbols show creep at $16\,\mathrm{MPa}$ with normal and inverse transient creep. Right panel: Creep rates for the $16\,\mathrm{MPa}$ stages; the values converge to the stationary rate.

The majority of tests is performed at elevated temperature (e.g. $60°\mathrm{C}$) to speed up the transient phases, and the activation energies are determined from supplementary tests at, e.g., $30°\mathrm{C}$ and $80°\mathrm{C}$.

All tests are conducted as triaxial tests at $20\ \mathrm{MPa}$ confining stress and include an isotropic consolidation phase of ten days.

4 Modified Procedure for Small Stress

Based on the understanding of creep mechanisms discussed in Section 1, it becomes clear that the procedure discussed in the previous section is only partially appropriate to stresses below $8\ \mathrm{MPa}$. While the consolidation phase and the accelerating influence of higher temperatures can be carried over, the two-stage tests with unloading are not helpful: Practically, an unloading by $2\ \mathrm{MPa}$ becomes too large for stresses of only a few MPa, and significantly smaller load steps, such as $0.2\ \mathrm{MPa}$, are experimentally challenging. Conceptually, the change of the dominant creep mechanism from dislocation motion to dissolution-precipitation processes implies much smaller transients and smaller stress exponents, so that the intersample scatter is likely to overwhelm the signal. Hence, the underlying motivation to use the transient creep stages to bound the stationary rates does not apply anymore.

In the WEIMOS project, we have adapted the approach for stresses above $8\ \mathrm{MPa}$ (Günther et al. 2015) to measure creep rates at low deviatoric stress:

- For the reasons discussed above, we use triaxial tests at high confining stress.
- Preexisting damage is reduced in an initial isotropic consolidation phase. It is recommended to monitor the creep rate and to continue the consolidation until the rate is small enough (e.g., significantly smaller than the expected creep rates in the first deviatoric load step).
- The consolidation phase and the first load stage are conducted at high temperature to speed up healing and transient creep, i.e. the evolution of the dislocation microstructure.
- The specified load is held until a stationary state is reached.
- In subsequent phases, the load is kept constant, and the temperature is reduced in steps of $20\ \mathrm{K}$. Since the dislocation structure only weakly depends on temperature, essentially no new transients occur, and later stages can be comparatively short.

With this procedure, we obtain several stationary rates, at fixed stress and several temperatures, from a single specimen. The time-consuming transient stage is accelerated by the initially high temperature and only happens once.

5 Long-Term Creep Test TCC34

We have performed a long-term creep test (TCC34) using the procedure discussed in the previous section. Sample material is clean salt from the Waste Isolation Pilot Plant (WIPP), see Figure 3, sample diameter and length are $60\ \mathrm{mm}$ and $120\ \mathrm{mm}$, respectively.

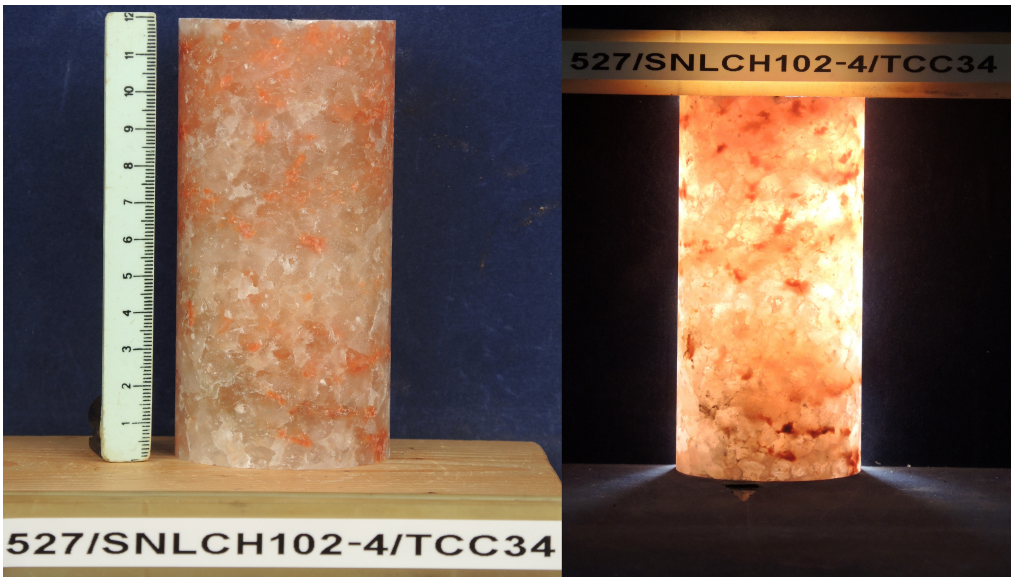


Figure 3: Sample for TCC34 (“clean salt” from WIPP; representative grain sizes in the range of several millimetres to a centimetre)

The test has been running for almost five years and is still ongoing. It started with two consolidation stages at an isotropic stress of $20\ \mathrm{MPa}$ at $298\ \mathrm{K}$ and $393\ \mathrm{K}$, with durations of about 50 and 80 days. The load of $4\ \mathrm{MPa}$ was applied by raising the axial stress (keeping the confining stress at $20\ \mathrm{MPa}$), the initial loading stage at $393\ \mathrm{K}$ ran for approximately 110 days. In the following stages, temperature was reduced to $373\ \mathrm{K}$, $353\ \mathrm{K}$, $333\ \mathrm{K}$, and $313\ \mathrm{K}$. To validate the underlying procedure, a number of steps was repeated afterwards – a temperature increase to $333\ \mathrm{K}$, a further isotropic stage and another loading at $4\ \mathrm{MPa}$, and two temperature stages at $353\ \mathrm{K}$ and $373\ \mathrm{K}$. The development of (true or logarithmic) strain over time is plotted in Figure 4. (In Figure 4 and later plots, dashed lines indicate isotropic-stress stages, solid lines stages with $4\ \mathrm{MPa}$ of deviatoric stress, and colours denote the temperature).

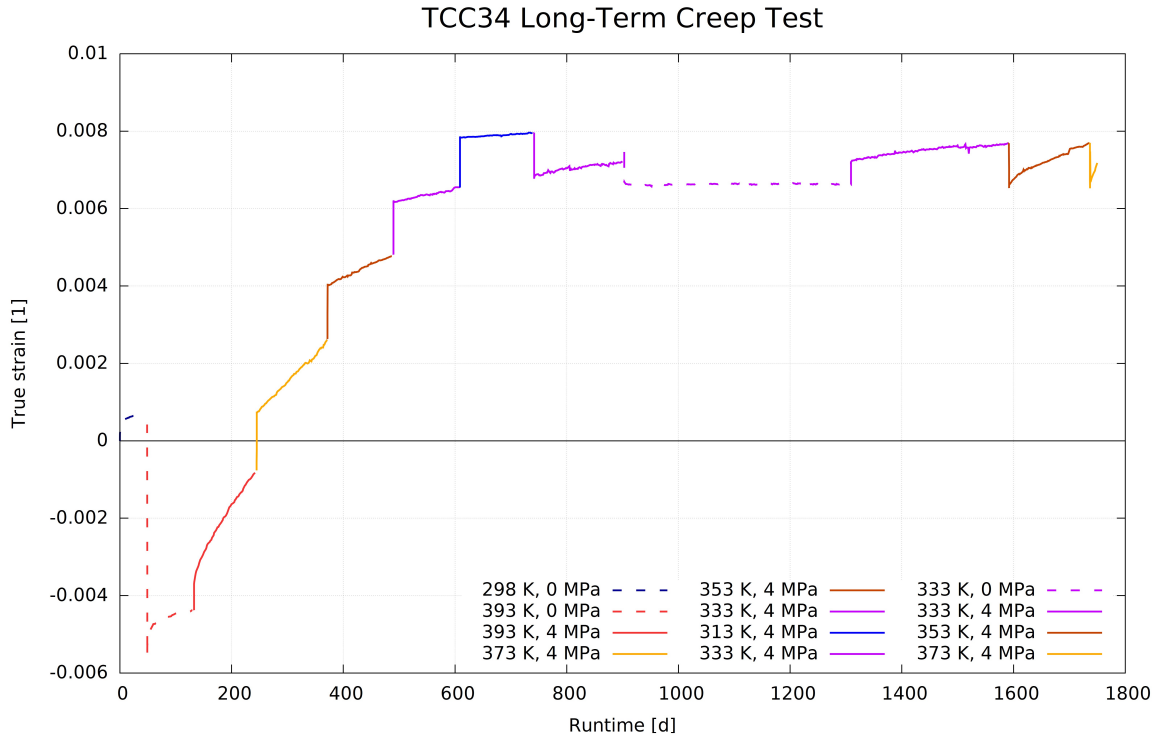


Figure 4: Deformation over time for TCC34.

In Figure 4, the deformation jumps at the points where the temperature changes due to the thermal expansion of sample and cell (the temperature changes take approximately seven hours). In Figure 5, the same data is plotted with temperature correction, showing only the creep deformation of the sample. Note that over 1750 days, the sample has accumulated a deformation of slightly more than 1%. The temperature dependence of the creep rate is clearly visible.

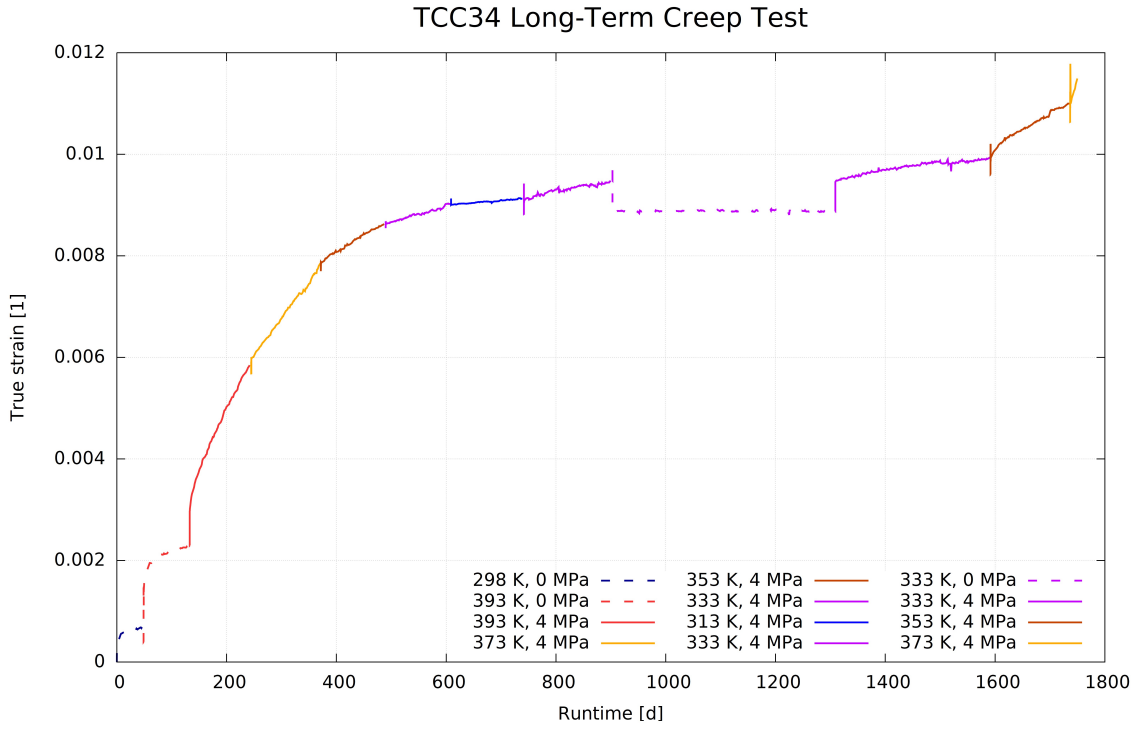


Figure 5: Temperature-corrected data for TCC34

To check the validity of the test procedure, we first analyse the isotropic phases. Figure 6 shows the consolidation and the second isotropic stage from $t = 903\ \mathrm{d}$ to $1309\ \mathrm{d}$. At the end of the consolidation phase, i.e. after more than 120 days, there is still a residual creep rate of $3.4 \times 10^{-6}/\mathrm{d} = 3.94 \times 10^{-11}/\mathrm{s}$. Note, however, that this is at $393\ \mathrm{K}$, and the stationary rate in the following load step is an order of magnitude larger at $2.04 \times 10^{-5}/\mathrm{d} = 2.36 \times 10^{-10}/\mathrm{s}$. In the second isotropic phase, there is no significant deformation anymore (note the small scale on the vertical axis in the right panel of Figure 6).

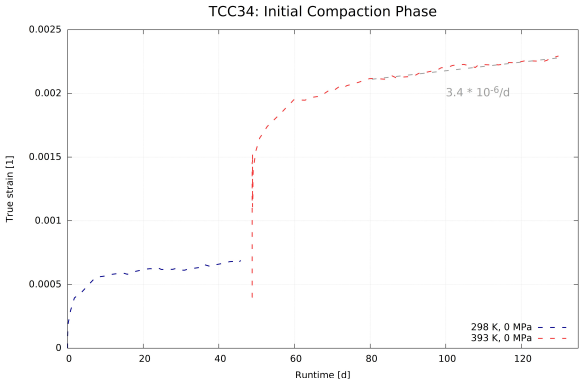


Figure 6: Isotropic phases of TCC34. Consolidation (left) and second phase (right).

During the test, there were two completed creep phases at $353\ \mathrm{K}$ and three at $333\ \mathrm{K}$. We should expect very similar creep rates with small transients; Figure 7 shows the results of the temperature stages, relative to the strain and time at the beginning of a given stage. The diagrams show that the individual stages line up well for both cases, except for a short transient phase of about 20 days for $353\ \mathrm{K}$.

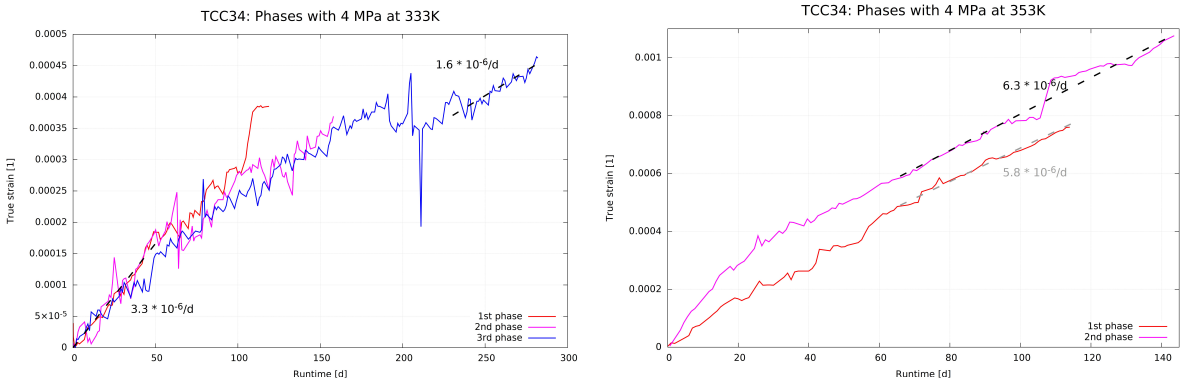


Figure 7: Phases with 333K (left), 353K (right)

We summarise the creep rates in Table 1.

Table 1: Creep rates at deviatoric stress of $4\ \mathrm{MPa}$ for different temperatures from long-term test TCC34

Temperature	Stationary creep rate	
K	$10^{-6}/\mathrm{d}$	$10^{-11}/\mathrm{s}$
393	20.4	23.6
373	15.0	17.4
353	6.3	7.29
333	1.6	1.85
313	0.96	1.11

To assess the temperature dependence, the Arrhenius plot is shown in Figure 8. The data points are to a good approximation described by a straight line corresponding to an activation energy of $42\ \mathrm{kJ/mol}$. Note that a value of $54\ \mathrm{kJ/mol}$, as it is often assumed for dislocation creep, is clearly disfavoured by the data. This is consistent with the transition from dislocation to dissolution-precipitation creep, for which an activation energy of $25\ \mathrm{kJ/mol}$ has been determined (in artificial crushed salt; Spiers et al. 1990). This, together with the clear transient phase in the first load stage, suggests that for a deviatoric stress of $4\ \mathrm{MPa}$ in the temperature range considered here, rock salt could be in the transition region where both dislocations and dissolution-precipitation contribute to creep deformation.

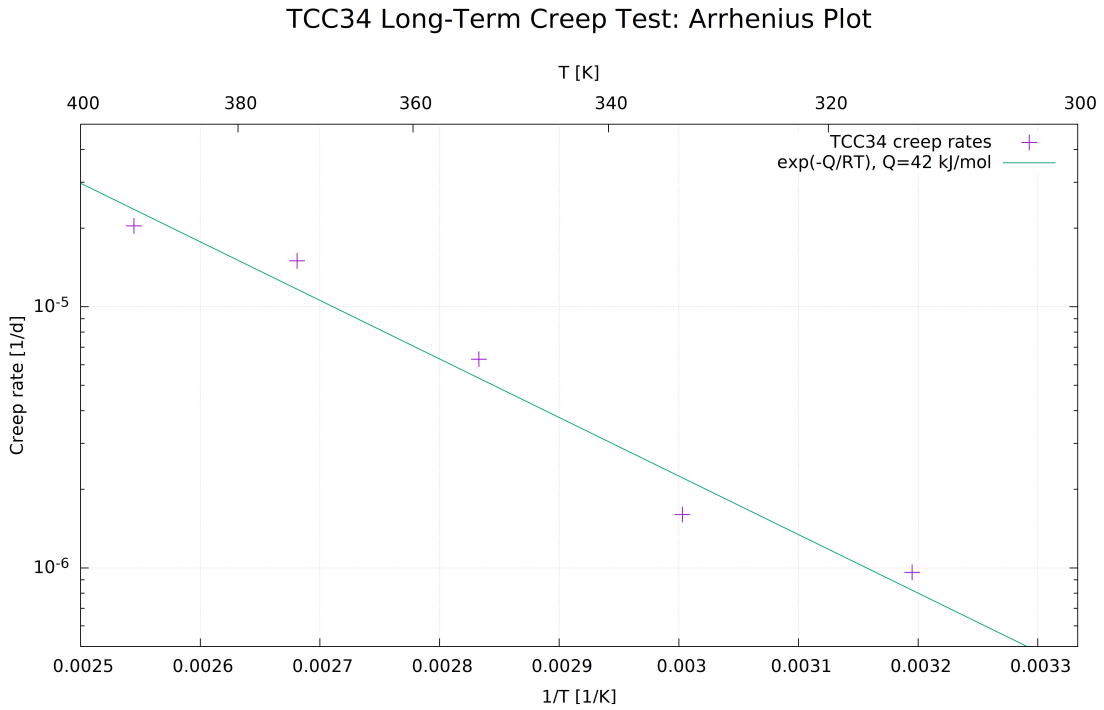


Figure 8: Logarithmic plot of the stationary creep rates versus inverse temperature. The temperature dependence of the creep rates is well described by an Arrhenius term with activation energy of $Q = 42\,\mathrm{kJ/mol}$.

6 Conclusions and Outlook

The long-term behaviour of waste repositories in rock salt, as well as that of mines and caverns, is dominated by creep at low deviatoric stresses, below, e.g., $6\,\mathrm{MPa}$ (Herchen et al. 2018; Hampel et al. 2022). However, the creep behaviour of natural rock salt is not well tested, and creep laws cannot be properly validated, in this range.

It is expected that for low stress, the dominant creep mechanism changes from dislocation motion to grain-boundary dissolution-precipitation processes (Carter et al. 1993; Hunsche, Schulze 1994; Urai et al 1986; Schleder, Urai 2005), which show a weaker stress and temperature dependence. The currently available data supports enhanced creep rates at low stress. However, data is scarce, and there are considerable uncertainties. Hence, while modern constitutive models include creep laws that allow for larger low-stress creep rates, a reliable derivation of parameter sets for specific rock salt varieties is currently not possible.

In this paper, we have presented an experimental procedure to measure creep rates at low stress. The key ingredients are

- triaxial tests at high confining stress to suppress dilatancy,
- an initial long isotropic compaction phase at high temperature to consolidate the sample,
- a first deviatoric load stage at high temperature to accelerate the transient phase,

- and subsequent temperature reduction steps at constant deviatoric stress to obtain several stationary creep rates from one sample.

Since the dislocation structure, which is primarily responsible for transient creep, only weakly depends on temperature, the later load stages show essentially no new transients. This test procedure should allow for a faster and more reliable determination of creep rates and activation energies in the low stress regime and thus help to validate creep laws and determine parameter sets. The long-term geomechanical behaviour of excavations in rock salt can thus be predicted with greater confidence.

We have performed a long-term test at a deviatoric stress of $4\ \mathrm{MPa}$. The results show that repeated stages are consistent and that there are only small transient phases. The test thus validates the proposed procedure.

Acknowledgements

The joint research project WEIMOS is funded by the German Federal Ministry for Economic Affairs and Energy (BMWI), with administrative support of the Project Management Agency Karlsruhe (PTKA-WTE).

References

BÉREST, P., H. GHARBI, B. BROUARD, G. HOFER, S. STIMMISHER, D. BRÜCKNER, K. DEVRIES, G. HÉVIN (2017) Very Slow Creep Tests as a Basis for Cavern Stability Analysis. SMRI Research Report RR2017-1

BÉREST, P., H. GHARBI, B. BROUARD, G. HOFER, S. STIMMISHER, D. BRÜCKNER, K. DEVRIES, G. HÉVIN, J. URAI, C. SPIERS, C. PEACH (2020) Very Slow Creep Tests as a Basis for Cavern Stability Analysis – Phase 2. SMRI Research Report RR2020-1

CARTER, N.L., S.T. HORSEMAN, J.E. RUSSELL, J. HANDIN (1993) Rheology of rocksalt. Journal of Structural Geology 15(9/10):1257-1271

GHARBI H., BÉREST P., BLANCO-MARTÍN L., BROUARD B. (2020). Determining upper and lower bounds for steady state strain rate during a creep test on a salt sample. Int. J. Rock Mech. Min. Sci. doi.org/10.1016/j.ijrmms.2020.104452

GÜNTHER, R.-M., K. SALZER, T. POPP, C. LÜDELING (2015) Steady-State Creep of Rock Salt: Improved Approaches for Lab Determination and Modelling. Rock Mech Rock Eng 48, 2603–2613 (2015). **https://doi.org/10.1007/s00603-015-0839-2**

HAMPEL, A., C. LÜDELING, R.-M. GÜNTHER, J.Q. SUN-KURCZINSKI, R. WOLTERS, U. DÜSTERLOH, K.-H. LUX, S. YILDIRIM, D. ZAPF, S. WACKER, I. EPKENHANS, J. STAHLMANN, B. REEDLUNN (2022). WEIMOS: Simulations of two geomechanical scenarios in rock salt resembling structures at WIPP. In: S. Hangx et al. (eds.), The Mechanical Behavior of Salt X. (this volume)

HERCHEN, K., T. POPP, U. DÜSTERLOH, K.-H. LUX, K. SALZER, C. LÜDELING, R.-M. GÜNTHER, C. RÖLKE, W. MINKLEY, A. HAMPEL, S. YILDIRIM, K. STAUDTMEISTER, A. GÄHRKEN, J. STAHLMANN, B. REEDLUNN, F.D. HANSEN (2018) WEIMOS: Laboratory Investigations of Damage Reduction and Creep at Small Deviatoric Stresses in Rock Salt. In: S. Fahland et al. (eds.), The Mechanical Behavior of Salt IX.

HUNSCHE, U., O. SCHULZE (1994) Das Kriechverhalten von Steinsalz. Kali und Steinsalz 11 (8/9) 1994

HUNSCHE, U., SCHULZE, O. (2002): Humidity induced creep and its relation to the dilatancy boundary. In: N.D. Cristescu, H.R. Hardy, Jr. & R.O. Simionescu (eds.): Basic and Applied Salt Mechanics, Proc. 5th Conf. on the Mechanical Behavior of Salt, Bucharest/Romania, 1999, pp. 73-87, Swets & Zeitlinger (A.A. Balkema Publishers), Lisse, ISBN 90 5809 383 2.

KOCK, I, EICKEMEIER, R., FRIELING, G, HEUSERMANN, S., KNAUTH, M., MINKLEY, W., NAVARRO, M., NIPP, H.-K., VOGEL, P. (2012) Integritätsanalyse der geologischen Barriere. Bericht zum Arbeitspaket 9.1. Vorläufige Sicherheitsanalyse für den Standort Gorleben. GRS-286. ISBN 978-3-939355-62-5. Gesellschaft für Anlagen- und Reaktorsicherheit (GRS) mbH, Köln.

LÜDELING, C., K. SALZER, R.-M. GÜNTHER, A. HAMPEL, S. YILDIRIM, K. STAUDTMEISTER, A. GÄHRKEN, J. STAHLMANN, K. HERCHEN, K.-H. LUX, B. REEDLUNN, S. SOBOLIK, F.D. HANSEN, S.A. BUCHHOLZ (2018) WEIMOS: Joint project on further development and qualification of the rock mechanical modelling for the final HLW disposal in rock salt Overview and first results on tensile stress modelling. In: S. Fahland et al. (eds.), The Mechanical Behavior of Salt IX.

MELLEGARD, K.D. & PFEIFLE, T.W. (1993). Creep Tests on Clean and Argillaceous Salt From the Waste Isolation Pilot Plant. Contractor Report, SAND92-7291, RE/Spec Inc., Rapid City, May 1993

REEDLUNN, B., ARGÜELLO, J.G., AND HANSEN F.D. (2022). A Reinvestigation into Munson's Model for Room Closure in Bedded Rock Salt. International Journal of Rock Mechanics and Mining Sciences. (Accepted)

SALZER, K., GÜNTHER, R.-M., MINKLEY, W., NAUMANN, D., POPP, T., HAMPEL, A., LUX, K.-H., HERCHEN, K., DÜSTERLOH, U., ARGÜELLO, J.G., HANSEN, F.D. (2015). Joint project III on the comparison of constitutive models for the mechanical behavior of rock salt, II. Extensive laboratory test program with clean salt from WIPP. L. Roberts, K. Mellegard & F. Hansen (eds.): The Mechanical Behavior of Salt; Proc. 8th Conference, South Dakota School of Mines & Technology, Rapid City, SD, USA, 26-28 May 2015, 3-12, Taylor &Francis Group, London, ISBN 978-1-138-02840-1.

SCHLEDER, Z., J.L. URAI (2005). Microstructural evolution of deformation- modified primary Halite from Hengelo, the Netherlands. International Journal of Earth Sciences 94(5-6): 941-956.

SPIERS, C.J., P. M. T. M. SCHUTJENS, R. H. BRZESOWSKY, C. J. PEACH, J. L. LIEZENBERG, H. J. ZWART (1990). Experimental determination of constitutive parameters governing creep of rocksalt by pressure solution, in: Deformation Mechanisms, Rheology and Tectonics, edited by R. J. Knipe, and E. H. Rutter, Geol. Soc. Spec Publ., 54, 215–227, 1990.

URAI, J.L., C.J. SPIERS, H.J. ZWART, G.S. LISTER, G.S. (1986). Weakening of Rock Salt by Water During Long-Term Creep. Nature 324: 554-557